Mem. S.A.It. Vol. 86, 241
© SAIt 2015
Memorie della

Looking for the traces of the early Universe in the Fornax dSph galaxy

A. del Pino Molina[1,2], S. L. Hidalgo[1,2], A. Aparicio[1,2], C. Gallart[1,2], R. Carrera[1,2], M. Monelli[1,2]

[1] Departamento de Astrofísica de Canarias, Universidad de La Laguna, E-38205, Tenerife, Spain
[2] Instituto de Astrofísica de Canarias, Calle Via Lactea, E-38205, La Laguna, tenerife, Spain, e-mail: adpm@iac.es

Abstract. We present the full Star Formation History as a function of radius of the Fornax dSph galaxy. We also present the preliminary results of the spatial distribution of the stellar populations. We found significant differences in the populations as a function of the galactocentric radius, which may be the result from interactions between Fornax and other systems. The implications of the obtained results on the dwarf spheroidal galaxies evolution are also discussed. This study is based on FORS1@VLT photometry as deep as I ∼24.5 and the IAC-star, IAC-pop and MinnIAC codes.

Key words. galaxies: evolution – Local Group – galaxies: dwarf – early Universe

1. Introduction

In the Λ-CDM scenario, dwarf galaxies are the building blocks from which larger galaxies are formed (e.g. Blumenthal et al. 1985; Dekel & Silk 1986; Navarro, Frenk & White 1995). The dwarf galaxies we observe today may be surviving systems that have not yet merged with larger galaxies. Hence, their underlying structure may provide important clues about the process of dwarf galaxy formation at high redshifts.

The evolution and star formation history (SFH) of dwarf galaxies are determined by local processes such as supernovae feedback and tidal interactions with nearby systems, as well as by global "*cosmic environmental factors*" like the reionization of the Universe by UV-background (Hayashi et al. 2003; Kravtsov et al. 2004; Kazantzidis et al. 2011). From one side, these global and local mechanisms could be responsible for suppressing galaxy formation in dwarf halos, and may explain the so called "*missing satellites problem*" (Klypin et al. 1999; Kazantzidis et al. 2004): simply, most of these satellites would be completely dark (Bullock et al. 2001). On the other hand, these effects could be involved in the large variety of properties in terms of mass, gas content, SFH, and chemical evolution that we observe today in dwarf galaxies.

The Local Group (LG) is a unique laboratory to study dwarf galaxies. The evolution of its member can be studied in a cosmological scale from the epoch of formation till the present time through the study of its stellar populations.

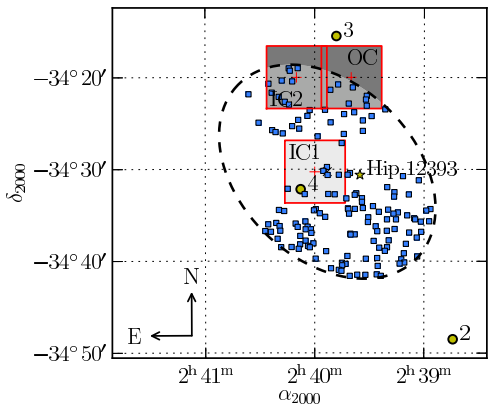

Fig. 1. Coverage of the photometry sets and the distribution of the CaT stars used for the spectroscopic AMR derivation. Solid lines show the boundaries of each observed field (squares). The regions defined for this work are represented in different gray shades and labelled accordingly. CaT stars are represented by small squares. The dashed ellipse corresponds to core radius of 13.8′ given by Mateo (1998). This ellipse defines a boundary for our radial bins. The yellow filled circles represent the position of the globular clusters 2, 3, and 4, which are labelled accordingly.

In the present work we present the full SFH of the Fornax dSph galaxy, and the preliminary results of the spatial distribution of its stellar populations. Fornax, one of the nine classic known dSph satellites of the Milky Way (MW), is a particularly important object. After the Sagittarius dSph, Fornax is the largest and most luminous of the spheroidal MW companions. These two galaxies are the only dSph satellites of the MW hosting globular clusters. Moreover, Fornax shows two conspicuous star clumps located at 17′ and at 1.3° from its centre that could be arised from an interaction with other system.

2. Data samples

We count on two different photometry sets (See Fig1). The first one consist in a wide field photometry list provided by Stetson (2000, 2005). With a limiting magnitude of $m_I \lesssim 23$, this photometry is not deep enough as to determine its SFH in detail, but its large coverage makes it perfect to study the spatial distribution of the differents stellar populations in Fornax. The second data set is a very deep FORS1@VLT photometry covering three fields located one at the centre, and the other two ∼10′ to the north. Reaching $m_I \lesssim 25$, this photometry allow us to obtain its detailed SFH.

3. Obtaining the SFH and the spatial distribution of stars

3.1. Wide field photometry

The color magnitude diagram (CMD) of Fornax provides substantial information about its stellar populations. We defined five regions in the CMD which typically contains stars within an age range. The sampling is as follow: (HB) the horizontal branch, populated very old stars (Age $\gtrsim 11-12$ Gyrs); (RGB) the red giant stars (Age $\gtrsim 1-2$ Gyrs); (RC) the intermediate-young aged stars of the red clump; (BP) the blue plume of the main sequence, which typically contains young stars (1 Gyr $\lesssim$ Age $\lesssim$ 2 Gyrs), and (BBP) the bluest and brightest stars of the main sequence.

In order to obtain the spatial distribution maps of the stars, we computed a 2 dimensional histogram of 142 × 128 pixels for stars within each defined CMD region. The density maps are normalized and convolved with a gaussian filter to reduce statistical noise.

3.2. Deep photometry

The position of our deep fields allows us to study the SFH as a function of the distance to the galactic centre. We defined three different regions for our study: IC1, IC2, and OC. The core radius ellipse given by Mateo (1998) was used to delimit our regions (See Fig1).

To solve the SFH in the three regions we followed the method developed by Aparicio & Hidalgo (2009). It is based on the SFH reconstruction by synthetic CMDs fitting techniques. Futher details about the followed procedure can be found in Hidalgo et al. (2011) and in del Pino et al. (2013).

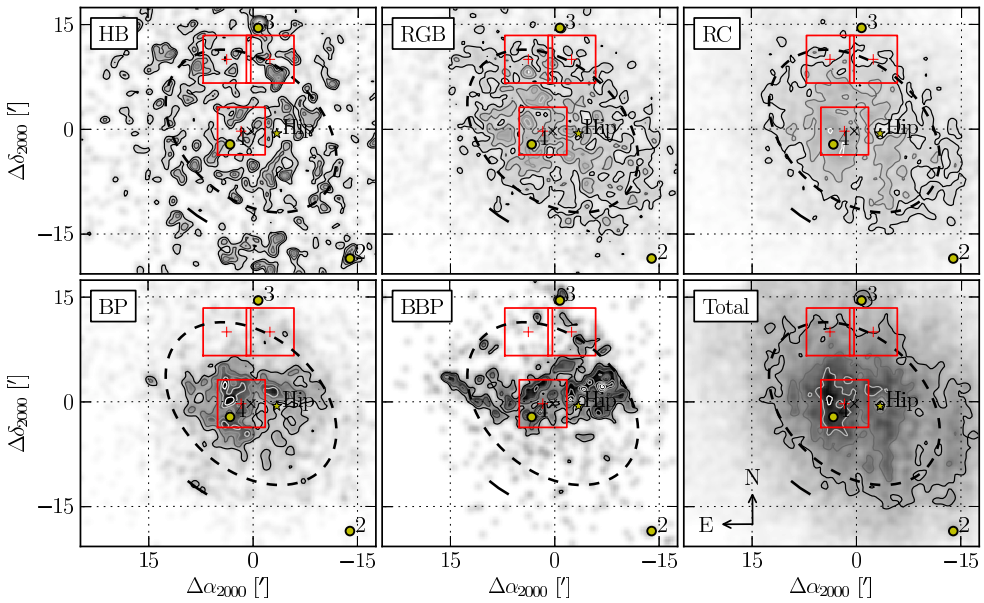

Fig. 2. Spatial distribution maps for the five defined populations in the CMD. Panels are ordered from old to young populations. Gray shade scale is common for all panels, and indicates the concentration of stars normalized to the number of stars of each population. Contours shows isodensities in multiples of the standart deviation for each population from 2σ.

4. Results

4.1. Spatial distribution

In Fig 2 we show the results of the spatial distribution of the stellar populations. Differences between populations are evident. We have found strong asymmetries in the young populations, with distributions which appear not to follow the orientation of the galactic axis, or even a spheroidal shape. Also noticeable is the shell previously detected by Coleman et al. (2004), which appear to be formed by stars of the BP, i.e. stars aged between 2 and 4 Gyrs. The oldest stars are uniformly spreaded well beyond the core radius, while stars from the RGB or the RC follow the spheroidal shape defined by the core radius.

4.2. The star formation history

Figure 3 summarizes the main results of ths SFH of the Fornax dSph. The innermost region (IC1) has the youngest stellar population of three regions, formed mainly by intermediate age stars. In the outer regions (IC2, OC) the importance of recent star formation episodes decrease gathering the bulk of their stars at old-intermediate ages. While outer regions shows a main burst occurred 10 Gyrs ago, the star formation in IC1 peaks ∼2 Gyrs latter.

4.3. The AMR comparison with CaT spectroscopy

It is worthy to compare our results with those derived from spectroscopy. In Figure 3 we have plotted the age-metallicity relation (AMR) of the Battaglia et al. (2006) sample. The stellar ages for these stars have been derived using the relationships by Carrera et al. (2008a,b). The agreement between the spectroscopy based AMR and the one obtained using photometry is very good in general, in all the cases.

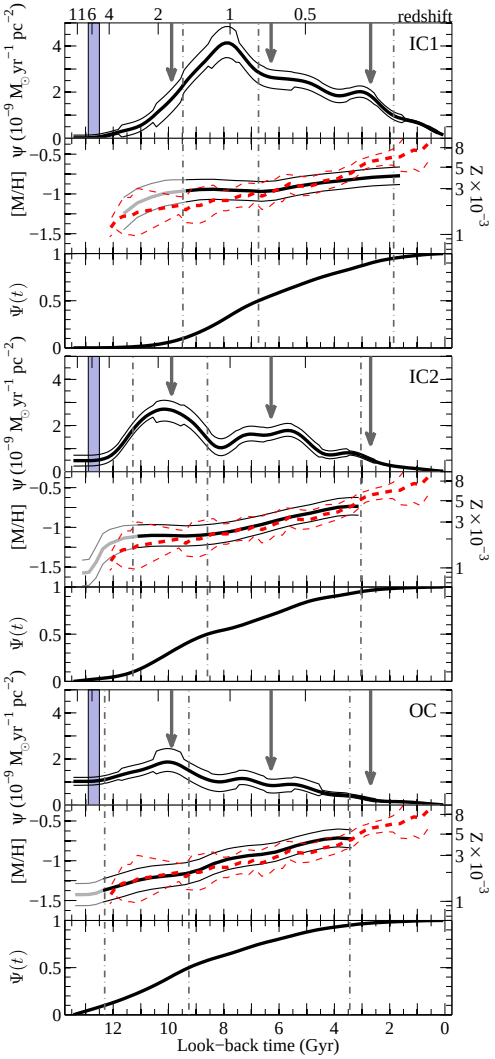

Fig. 3. Star formation rate as a function of time ($\psi(t)$) (upper panel), age-metallicity relation (middle panel), and the cumulative mass fraction, $\Psi(t)$, (bottom panel) of each region. Errors are drawn by thin lines. Plots are ordered from top to bottom: IC1, IC2, and OC respectively. Units of $\psi(t)$ are normalized to the corresponding region area. 10th,50th, and 95th-percentile of $\Psi(t)$ are drawn with dash-dotted vertical lines. A redshift scale is given in the upper axis. Reionization era is marked at $z \sim 6$ in blue. The AMR obtained from CaT spectroscopy is represented by a red-dashed line. Possible passes of Fornax through it perigalacticon, derived from the orbital parameters by Piatek et al. (2007), are represented by vertical arrows.

5. Conclusions

Fornax is a complex system with strong differences between its stellar populations. It shows the most recent star formation events of any Local Group dSph. We find evidence for Fornax stars as young as ≤1 Gyr, while the first star formation event occurred at the oldest epoch (∼ 12 Gyrs ago). Last star formation events are mainly located in the central region of the galaxy. Moving outside, the fraction of young stars decrease, leaving old metal-poor stars as the dominant population. This may indicate that gas reservoir in the outer parts of the galaxy would be exhausted earlier in these regions than in the centre or that it was removed due to interacions with others systems.

We have derived the AMR for Fornax dSph following two completely different methods with different data (Photometry and CaT spectroscopy) obtaining the same result for both of them. The latter is an important result since not only proves the reliability of the method, but also suggest that it can be applied in systems in which obtain spectroscopy would be difficult. Fornax has formed approximately the 90% of its stars after UV-reionization, and has retained gas against SNe feedback.

References

Aparicio, A. & Hidalgo, S. L. 2009, AJ, 138, 558
Battaglia, G., et al. 2006, A&A, 459, 423
Blumenthal, G. R., et al. 1985, Nature, 313, 72
Bullock, J. S., et al. 2001, ApJ, 548, 33
Carrera, R., et al. 2008b, AJ, 136, 1039
Carrera, R., et al. 2008a, AJ, 135, 836
Coleman, M., et al. 2004, AJ, 127, 832
Dekel, A., & Silk, J. 1986, ApJ, 303, 39
Hayashi, E., et al. 2003, ApJ, 584, 541
Hidalgo, S. L., et al. 2011, ApJ, 730, 14
Kazantzidis, S., et al. 2004, ApJ, 608, 663
Kazantzidis, S., et al. 2011, ApJ, 726, 98
Klypin, A., et al. 1999, ApJ, 522, 82
Kravtsov, A. V., et al. 2004, ApJ, 609, 482
Mateo, M. L., 1998, ARA&A, 36, 435
Navarro, J. F., et al. 1995, MNRAS, 275, 720
Piatek, S., et al. 2007, AJ, 133, 818
del Pino, A., et al. 2013, MNRAS, 433, 1505
Stetson, P. B. 2000, PASP, 112, 925
Stetson, P. B. 2005, PASP, 117, 563